

## CHAPTER 8

---

# Kinetic Proofreading Model

Byron Goldstein,\* Daniel Coombs, James R. Faeder and William S. Hlavacek

### Abstract

**K**inetic proofreading is an intrinsic property of the cell signaling process. It arises as a consequence of the multiple interactions that occur after a ligand triggers a receptor to initiate a signaling cascade and it ensures that false signals do not propagate to completion. In order for an active signaling complex to form after a ligand binds to a cell surface receptor, a sequence of binding and phosphorylation events must occur that are rapidly reversed if the ligand dissociates from the receptor. This gives rise to a mechanism by which cells can discriminate among ligands that bind to the same receptor but form ligand-receptor complexes with different lifetimes. We review experiments designed to test for kinetic proofreading and models that exhibit kinetic proofreading.

### Introduction

For many receptors the occupancy of their binding sites by the appropriate ligand is insufficient to initiate a cellular response; rather these receptors must aggregate with additional membrane proteins or among themselves to initiate a signal. As exemplified by the multichain immune recognition receptors (MIRRs), transmitting information across the cell membrane by juxtaposing the cytoplasmic tails of receptors is a common signaling mechanism used in every facet of immune system function. The subunits of the MIRRs can be divided into those that participate in binding and those that participate in signaling. All the signaling subunits, but none of the binding subunits, have at least one copy of a common sequence motif, an immunoreceptor tyrosine-based activation motif (ITAM) in their cytoplasmic domains. Each ITAM is composed of a pair of YXXL/I sequences usually separated by seven or eight amino acid residues.<sup>1,2</sup> Upon receptor aggregation, ITAM tyrosines become phosphorylated. It is by converting cytoplasmic domains of the receptor to phosphorylated forms that the cell first “senses” the external ligand and a signaling cascade is initiated.

The cell synthesizes information during signal transduction through chemical reactions that build and use transient molecular scaffolds. The cytoplasmic domains of the receptors and other scaffolding proteins are sites for coalescence of kinases, phosphatases and adapters. The structures formed are ephemeral with components going on and off rapidly. Completion of construction depends on the lifetime of the receptor-ligand complex. If the lifetime of the complex is too short, most of the chemical cascades that are initiated will fail to go to completion, the signaling will be aborted and no response will be produced. This is the essence of kinetic proofreading, an idea introduced by Hopfield<sup>3,4</sup> to explain how high specificity arises in biosynthetic pathways and resurrected in the context of cell signaling by McKeithan,<sup>5</sup> who proposed it as a mechanism to explain how T-cell antigen receptors (TCRs) discriminate between foreign and self-antigens.

---

\*Corresponding Author: Byron Goldstein—Theoretical Biology and Biophysics Group, T-10 MS K710, Theoretical Division, Los Alamos National Laboratory, Los Alamos, NM 875435, USA.  
Email: bxg@lanl.gov

## Kinetic Proofreading Illustrated through FcεRI Signaling

The clearest demonstration of kinetic proofreading in cell signaling used ligands of low valence with different dissociation rate constants to aggregate high-affinity IgE receptor FcεRI on mast cells and trigger downstream responses.<sup>6</sup> We will review this experimental work but first we will illustrate kinetic proofreading using a detailed mathematical model of the initial signaling cascade mediated by FcεRI.<sup>7</sup> The beauty of using such a model is that we know exactly what is in the model, which molecules make up the chemical network and how they interact and we can pick the perfect ligands and concentrations to test our ideas.

In Figure 1, we review how FcεRI ITAMs become phosphorylated, how this leads to the recruitment of the protein tyrosine kinase (PTK) Syk from the cytosol and how Syk then becomes

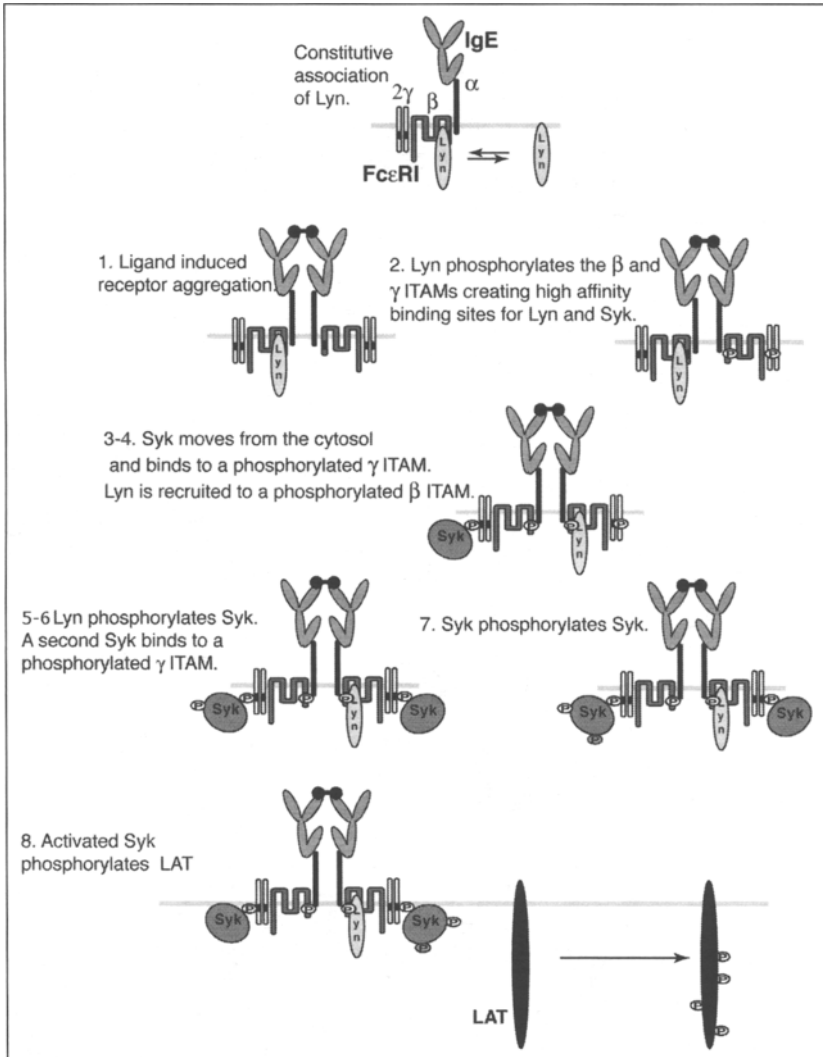


Figure 1. Initial steps in FcεRI signaling. FcεRI is a four chain MIRR. The α chain binds IgE with high affinity. The β and two γ chains participate in signaling and each contain a single ITAM. In the basal state, the Src kinase Lyn constitutively associates with the unphosphorylated β chain.<sup>11,12</sup>

activated. All the reactions shown in Figure 1 are included in the mathematical model. Briefly, the initiating Src family kinase Lyn constitutively associates with the  $\beta$  chain of the receptor. Upon receptor aggregation, if Lyn is present in an aggregate, it can transphosphorylate both the  $\beta$  and  $\gamma$  ITAM tyrosines. The amount of Lyn available to the receptor in rat basophilic leukemia (RBL) cells is limiting, so that often (at least in this cell line) receptor aggregates initially contain no Lyn.<sup>8-10</sup> In the basal state, the Src kinase Lyn constitutively associates with the unphosphorylated  $\beta$  chain.<sup>11,12</sup> Lyn can bind through its single SH2 domain to a phosphorylated  $\beta$  ITAM while Syk, with two SH2 domains, can form a stable complex with a  $\gamma$  chain ITAM only when both of the ITAM tyrosines are phosphorylated.<sup>13,14</sup> Syk is phosphorylated on multiple tyrosines by both Lyn and Syk.<sup>15,16</sup> Syk is fully activated when the two tyrosines in its activation loop, Tyr519 and Tyr 520, are phosphorylated.<sup>17,18</sup> The roles of the specific tyrosines of Syk are reviewed in ref. 18. In the model, all the phosphorylation reactions that take place at the receptor are trans, i.e., Lyn and Syk cannot phosphorylate substrates that are associated with any of the chains of the receptors they are associated with. Transphosphorylation of the receptor by Lyn has been demonstrated<sup>19</sup> and there is indirect evidence that Syk phosphorylation of Syk is trans as well.<sup>15</sup> In the model, this is assumed and thus two Syk molecules must be simultaneously associated with a receptor aggregate for a Syk to transphosphorylate the activation loop of an adjacent Syk. Whether signaling proceeds depends to a large extent on the competition between kinases and phosphatases. Even while receptors are held in an aggregate, they are constantly undergoing phosphorylation and dephosphorylation with kinases and phosphatases moving in and out of the aggregate.<sup>20,21</sup> When a receptor leaves an aggregate and is separated from the kinase that is phosphorylating its ITAMs, it undergoes rapid dephosphorylation.<sup>22</sup> In the mathematical model, a pool of unspecified protein tyrosine phosphatases account for the dephosphorylation reactions.

A detailed description of the model along with all the parameters and how they were obtained is given in Faeder et al.<sup>7</sup> The model consists of the receptor, Fc $\epsilon$ RI, a bivalent ligand that can only aggregate receptors into dimers (higher aggregates can't form), the PTKs Lyn and Syk, and a background pool of phosphatases. The model describes the association, dissociation, phosphorylation and dephosphorylation among the components. In the model, these reactions can lead to 354 distinct chemical species. Using software called BioNetGen (<http://bionetgen.janl.gov/>) that was developed to build cell signaling models,<sup>23,24</sup> 354 ordinary differential equations can be generated whose solutions give the concentrations of each chemical species as a function of time. Although we can look at the time courses of all 354 chemical species,<sup>25</sup> the most useful outputs of the model usually correspond to experimentally determined quantities. For example, if we are interested in how the phosphorylation of the  $\beta$  ITAM changes in time, we add up the time courses of all the concentrations of the chemical species that have the  $\beta$  ITAM phosphorylated, a few of which are shown in Figure 2. We can then predict how the phosphorylation of the  $\beta$  ITAM changes in time after the addition of the bivalent ligand.

To see if this network model of the early events of Fc $\epsilon$ RI-mediated cell signaling exhibits kinetic proofreading, we take as our ligands three monoclonal anti-Fc $\epsilon$ RI that aggregate Fc $\epsilon$ RI into dimers (Fig. 3). We take these ligands to have the same forward rate constants,  $k_{+1}$  and  $k_{+2}$ , but to differ in their reverse rate constants,  $k_{-1}$  and  $k_{-2}$ . Note that the mean lifetime of a receptor

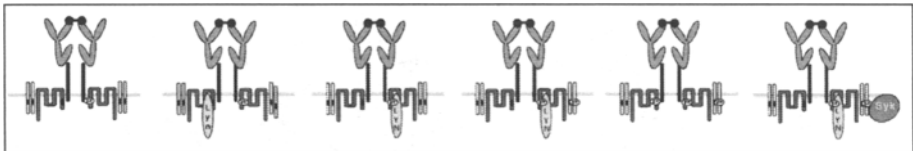


Figure 2. Six of the 170 chemical species in the model that have at least one  $\beta$  ITAM phosphorylated. The model lumps the two ITAM tyrosines together so that an ITAM is either phosphorylated or not phosphorylated.

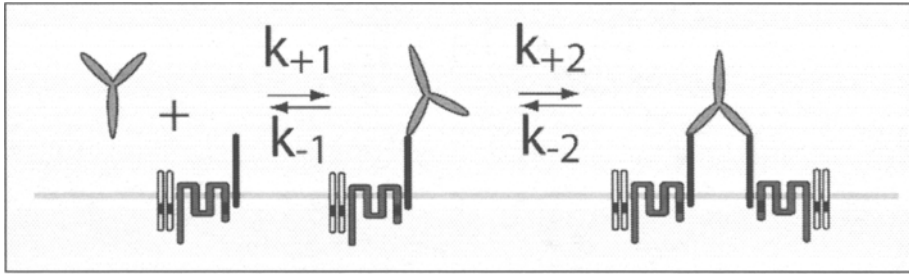


Figure 3. Kinetic scheme for the binding of an anti-IgE $\alpha$  monoclonal antibody to an Fc $\epsilon$ RI.

in a dimer formed by a monoclonal antibody bridging two Fc $\epsilon$ RI is  $1/k_{-2}$ . In the simulations, we take the value of  $k_{-2}$  for the three ligands to be  $0.05 \text{ s}^{-1}$ ,  $0.5 \text{ s}^{-1}$  and  $5 \text{ s}^{-1}$ .

Shown in Figure 4 are the predicted levels of  $\beta$  and  $\gamma$  ITAM phosphorylation and Syk autophosphorylation (Syk is phosphorylated in its activation loop by another Syk) at long times when the model has reached a steady state. Because none of the components in the model are downregulated, the model goes to a steady state with a distribution of chemical species populated. These quantities are plotted as a function of the number of Fc $\epsilon$ RI in aggregates. From Figure 4, we can compare the responses induced by the three ligands when they form the same number of aggregates on the cell surface. For example, for the vertical dotted line in Figure 4, all the ligands maintain 3000 dimers on the cell surface in the steady state. To achieve this number of dimers, the ligand concentration for the most rapidly dissociating ligand is about 100-fold higher than the ligand with the intermediate dissociation rate, whose concentration is in turn about 100-fold higher than the slowest dissociating ligand (see the three horizontal dotted lines in Fig. 4). As can be seen, there is little difference in the amount of  $\beta$  and  $\gamma$  ITAM phosphorylation induced by the ligand but for the response furthest downstream in our model, the autophosphorylation of Syk, there is a dramatic difference in the response to the three ligands. This is a manifestation of kinetic proofreading, where the lifetime of the receptor in an aggregate strongly influences downstream responses. In summary, the model shows that a rapidly dissociating ligand will often be less effective in generating a response than a slowly dissociating ligand, even when the ligand concentrations are chosen to give the same number of receptors in aggregates.

As illustrated in Figure 5, higher ligand concentrations can compensate for faster rates of dissociation up to a point. For the slowest and intermediate dissociating ligands one can choose concentrations for each,  $3 \times 10^{-8} \text{ M}$  and  $2 \times 10^{-11} \text{ M}$ , respectively, that induce 1000 molecules per cell of autophosphorylated Syk. If there were no further proofreading downstream of Syk, then we would expect these ligands at the two different concentrations to produce similar, but probably not identical, cellular responses. Since the time course of binding and formation of receptor aggregates differ for the two ligands, the time courses of the responses and possibly their magnitudes might differ as well. We will address the question of whether there is further proofreading beyond Syk shortly.

To test for kinetic proofreading experimentally, Torigoe et al<sup>6</sup> compared the time courses of cellular responses triggered by rapidly and slowly dissociating multivalent ligands that bound to and aggregated a monoclonal anti-2,4-dinitrophenyl (DNP) IgE. RBL cells were sensitized with anti-DNP IgE, creating long-lived complexes of anti-DNP IgE and Fc $\epsilon$ RI on the cell surface. The concentrations of the two ligands were adjusted so that the rapidly dissociating ligand induced a maximal receptor phosphorylation (the sum of  $\beta$  and  $\gamma$  ITAM phosphorylation) that was twice that of the slowly dissociating ligand. Figure 6 shows that the rapidly dissociating ligand was progressively less effective in stimulating downstream events. The experiments permit comparison between the relative phosphorylation levels of each protein induced by the two ligands, but do not permit comparison between the phosphorylation levels of different proteins. As seen in Figure 6, the maximum phosphorylation of Syk induced by the rapidly dissociating ligand was less than

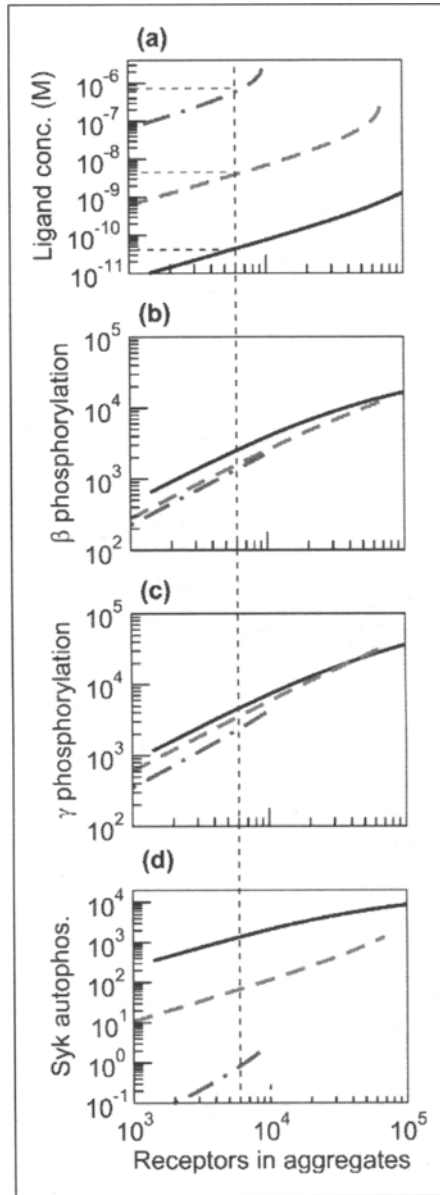


Figure 4. Simulation using a network model for three monoclonal anti-Fc $\epsilon$ RI $\alpha$  that aggregate receptors only into dimers. The figure is modified from Figure 8 of Faeder et al (2003) where all the parameters values for the simulation are given. The values plotted are obtained at steady state. For the three ligands, the forward rate constants are taken to be the same at  $k_{f1} = 10^6 \text{ M}^{-1} \text{ s}^{-1}$  and  $k_{f2}R_T = 0.5 \text{ s}^{-1}$  where  $R_T$  is the RBL surface concentration of Fc $\epsilon$ RI. The reverse rate constants,  $k_{r1} = k_{r2}$ , have the following values:  $0.05 \text{ s}^{-1}$  (black solid lines),  $0.5 \text{ s}^{-1}$  (red dashed lines) and  $5.0 \text{ s}^{-1}$  (blue dash-dot lines). The x axis is in number of receptors in aggregates. (a) Ligand concentration required to achieve given levels of aggregation, (b) number of receptors per cell with the  $\beta$  ITAM phosphorylated, (c) number of receptors per cell with the  $\gamma$  ITAM phosphorylated and (d) number of autophosphorylated Syk per cell. Modified from a figure in *J Immunol*.

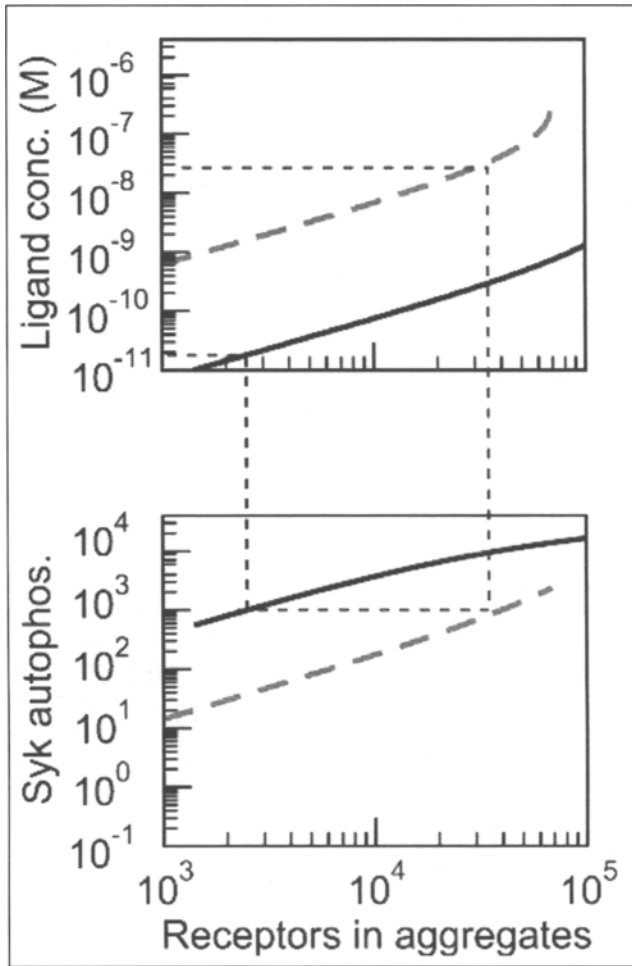


Figure 5. The two panels from Figure 4 with the results for the rapidly dissociating ligand,  $k_{-1} = 5.0 \text{ s}^{-1}$ , omitted. Over a limited range higher ligand concentrations can compensate for faster rates of dissociation. Concentrations for the two ligands (top panel) can be found so that both activate 1000 Syk molecules per cell (bottom panel). Modified from a figure in *J Immunol*.

one-third of that induced by the slowly dissociating ligand. Follow up experiments confirmed these results for Syk.<sup>26</sup> For Erk phosphorylation, which is known to be downstream of Syk, the ratio of the maximal responses was about a tenth. From these experiments, Torigoe et al<sup>6</sup> concluded that “these findings are consistent with a kinetic proofreading regime.”

Although the experiments are consistent with the predictions of kinetic proofreading, a feature of cell signaling not controlled for in these experiments was the level of phosphorylation of the individual tyrosines in the  $\beta$  and  $\gamma$  ITAMs of the receptors. Even though the receptors on RBL cells exposed to the rapidly dissociating ligand had maximum levels of total receptor phosphorylation that were higher than for the receptors on cells exposed to the slowly dissociating ligand, the distribution of phosphorylated tyrosines for these two cases may have been quite different. If that were the case, the differences in downstream signaling could result from different patterns of tyrosine phosphorylation rather than the different rates of dissociation. Simulations of the model

indeed show that  $\gamma$  and  $\beta$  phosphorylation exhibits different behaviors as the ligand dissociation rate is varied,<sup>38</sup> but this relatively small difference does not account for the dramatic reduction of Syk phosphorylation at higher dissociation rates (Fig. 4d). Experiments also show that the ratio of  $\gamma/\beta$  phosphorylation changes as the ligand dissociation rate increases,<sup>51</sup> but these differences seem unlikely to account for the full extent of the decrease in downstream activation events. Because the  $\beta$  and  $\gamma$  ITAMs contain 3 and 2 tyrosines respectively, it would be necessary to repeat these studies using site-specific anti-phosphotyrosine antibodies to fully resolve the effects of differential phosphorylation of individual tyrosines and ITAMs.

### The Extent of Kinetic Proofreading in Fc $\epsilon$ RI Signaling

A major function of activated Syk associated with Fc $\epsilon$ RI is to phosphorylate the transmembrane adaptor protein linker for activation of T-cells (LAT).<sup>27</sup> When receptor aggregates are broken up by adding large amounts of hapten that compete for IgE-binding sites with the ligand responsible for receptor aggregation, LAT is rapidly dephosphorylated.<sup>28</sup> The present view is that LAT phosphorylation is maintained through enzyme-substrate reactions involving transient associations of LAT with activated Syk- Fc $\epsilon$ RI complexes. These reactions are thought to occur predominantly in specialized lipid domains where LAT is preferentially located<sup>29</sup> and where aggregated receptors tend to cluster,<sup>30-32</sup> although electron microscopy suggests a more complex topographical organization of membrane microdomains.<sup>33</sup> If the lifetime of the association of activated Syk with LAT is short compared to the lifetime of a receptor in an aggregate, then we expect events that stem from LAT phosphorylation not to be subject to kinetic proofreading. The experiments of Torigoe et al<sup>6</sup> suggest a way to test this idea—use the same rapidly and slowly dissociating ligands but choose concentrations such that the two ligands induce the same level of LAT phosphorylation, then see if downstream events still show signs of kinetic proofreading. Counter to what we anticipated, our results were consistent with kinetic proofreading beyond LAT phosphorylation.<sup>52</sup> In these experiments, however, although the overall level of LAT phosphorylation was the same, the pattern of LAT phosphorylation was not determined, leaving open the possibility that differences in the phosphorylation pattern could be responsible for the apparent proofreading.

### Some Responses May Escape Kinetic Proofreading

Although many cellular responses are subject to kinetic proofreading some responses have been observed that appear to “escape” kinetic proofreading.<sup>26,34,35</sup> The same rapidly and slowly dissociating ligands used by Torigoe et al<sup>6</sup> to detect kinetic proofreading were subsequently found to

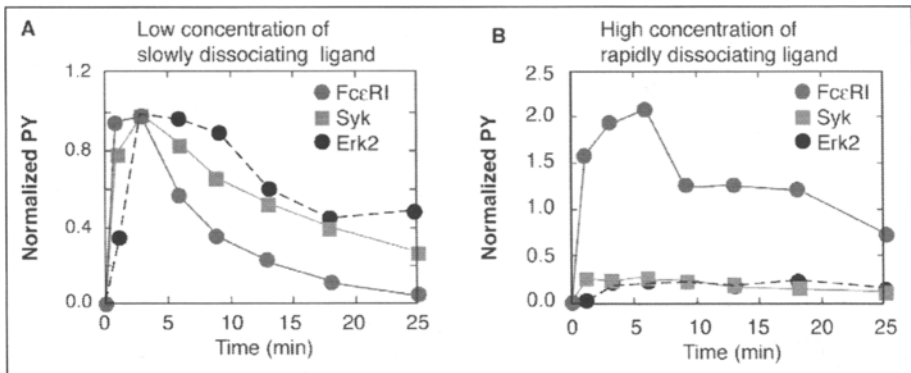


Figure 6. Time course of phosphorylation of several proteins in RBL cells sensitized with anti-DNP IgE after stimulation with (A) a slowly dissociating (high affinity) DNP-conjugated antigen (50 ng/ml) or (B) a rapidly dissociating (low affinity) 2NP-conjugated antigen (375 ng/ml). Adapted from Science: Torigoe C, Inman JK and Metzger H. An unusual mechanism for ligand antagonism. Science 1998; 281:568-72.

stimulate the transcription of the gene for monocyte chemoattractant protein-1 (MCP-1) to about the same extent. Even though this is a late response and one might think it should be subject to many proofreading steps, it appears that that is not the case. To explain how a cellular response might avoid kinetic proofreading, a mechanism was proposed in which a soluble “messenger” generated early in the chain of chemical modifications that follow receptor aggregation determines the response. To investigate this idea, McKeithan’s<sup>5</sup> mathematical formulation of kinetic proofreading (see below) was extended to allow a branch reaction in which a modified receptor, one that has associated with appropriate signaling molecules, acts as an enzyme on an intracellular substrate to generate a messenger.<sup>36,37</sup> If the response saturates as a function of the messenger concentration, then even if the rapidly dissociating ligand leads to the production of less messenger than the slowly dissociating ligand, both amounts may be sufficient to produce the same response. If this is the mechanism, then at lower concentrations of both ligands, when the rapidly dissociating ligand produces message below the saturating level, kinetic proofreading should once again be observed as it is for the production of mRNA for MCP-1.<sup>26</sup> In general, if a response saturates with respect to the level of an intermediate messenger, kinetic proofreading may be masked at high ligand concentrations but be revealed at low concentrations.

### McKeithan’s Mathematical Formulation

McKeithan<sup>5</sup> introduced a simple mathematical model to explain how the binding properties of peptide-MHC (pMHC) for the TCR influence the activation of the TCR (reviewed in refs. 38 and 39). According to the model, a bound receptor must complete a series of modifications to generate a cellular response. The model replaces the complex chemistry of the signaling cascade by a linear sequence of reactions but tries to capture a basic feature of the signaling process, that multiple events unspecified in the model must happen for the TCR to become activated. The series of modifications can be thought of as representing intermediate steps, such as the steps required for the formation of the scaffolding about the receptor and LAT. If the ligand dissociates before all the modifications have occurred, the receptor reverts to its basal state and no productive signal results as, for example, when FcεRI dissociates from aggregates and rapidly undergoes dephosphorylation.<sup>22</sup> An attractive feature of the model, illustrated in Figure 7, is that minor differences in the lifetime of a TCR-pMHC complex lead to huge differences in TCR-mediated signaling.

Since McKeithan<sup>5</sup> introduced his model, the view of the surface events that drive T-cell activation has changed. At low agonist pMHC surface concentrations, it appears that agonist/endogenous pMHC heterodimers act as the signaling unit that initiates T-cell signaling.<sup>40</sup> Thus, it might be useful to generalize the model to include endogenous pMHC and heterodimer formation, but as we discuss below, the main weakness of the McKeithan model and extended versions considered so far is the overly simplistic way in which signaling is treated.

There are four parameters in the McKeithan model, the forward and reverse rate constants for binding and dissociation of the pMHC to and from the TCR in the immunological synapse,  $k_{+1}$  and  $k_{-1}$  and the parameters that characterize the signaling events,  $k_p$  and  $N$ . From Figure 7, we see that in the model,  $N$  is the number of successive, irreversible modifications a bound TCR must complete to become activated and  $k_p$  is the rate constant for each modification. The difficulty is that the model does not specify how to determine these parameters from experiment and as a result, the model cannot make testable quantitative predictions. At the heart of the problem is the replacement of a highly branched biochemical network with a linear chain of reactions. Not surprisingly, there is no clear correspondence between the model parameter  $k_p$  and the set of reaction rates in the chemical cascade nor between  $N$  and the average number of reactions that occur for receptor activation. In the model  $N/k_p$  is the mean time for a receptor to become activated so we can put an estimate on this quantity,  $N/k_p$ . If we are interested in a rapid response, such as the activation of ZAP-70, it is probably of order seconds, whereas if we are interested in late response, such as IL-2 production, it might be hours.



## T-Cell Activation and the Competition between Kinetic Proofreading and Serial Engagement

Despite its shortcomings, the McKeithan model has been used to make interesting qualitative predictions. The most investigated of these concerns the implications of the competition between kinetic proofreading and serial engagement (Chapter 9 and Valitutti et al<sup>41</sup>). To achieve a robust T-cell response, the activation of many TCRs is required. Kinetic proofreading works at the level of the individual receptor and to become activated, a TCR bound to a pMHC must complete a series of biochemical modifications before dissociating from the pMHC. Thus, the half-life of the pMHC-TCR complex must be long enough to allow completion of the signaling events required for TCR activation. Under physiological conditions, the density of cognate pMHC on antigen-presenting cells (APCs) is low. Thus, the half-life of the pMHC-TCR complex must be short enough to permit a single peptide to bind and dissociate many times, i.e., to serially engage multiple TCRs. The recognition that there is a trade off between kinetic proofreading and serial engagement led to the proposal that there is an optimal pMHC-TCR half-life for T-cell activation.<sup>41-44</sup> One way to see this is to look at the initial rate of TCR activation after synapse formation.

$$\text{activation rate} = (\text{hits/s}) \times (\text{fraction activated}) \quad (1)$$

By hitting rate (hits/s) we mean the rate at which a single pMHC engages TCRs. In the absence of TCR internalization, or if internalization of TCR only occurs when a TCR is not bound to pMHC, the rate of serial engagement per pMHC is<sup>44,45</sup>

$$\text{hits/s} = 1/(1/k_{-1} + 1/(k_{+1}T)) = k_{+1}KT/(1+KT) \quad (2)$$

where  $K = k_{+1}/k_{-1}$  is the two-dimensional equilibrium constant  $K$  for binding in the immunological synapse of pMHC on an APC to a TCR on a T-cell and  $T$  is the concentration of unbound TCR in the synapse. An assumption underlying Eq. (2) is that the density of cognate pMHC is small relative to the density of TCR so that individual pMHC do not compete for TCRs.

For the model in Figure 7, the fraction of pMHC-bound TCRs that go through all the steps leading to activation is

$$\text{fraction activated} = (k_p/(k_p + k_{-1}))^N \quad (3)$$

The initial activation rate, Eq. (1), therefore becomes

$$\text{activation rate} = (k_{+1}KT/(1+KT)) (k_p/(k_p + k_{-1}))^N \quad (4)$$

For even modest values of  $N$  the fraction of activated TCR can be quite sensitive to small variations in  $k_{-1}$ . For example, consider two pMHC-TCR complexes whose half-lives differ by a factor of 2. For  $N = 10$  and  $k_{-1}/k_p = 1$  and 2, respectively, the fractions activated are  $9.8 \times 10^{-4}$  and  $1.7 \times 10^{-5}$ , i.e., 57 times more TCRs are activated by the pMHC with the longer complex half-life. However, in the model this power of discrimination comes at the expense of the overall sensitivity to specific pMHC. To continue with our example, if  $k_{-1} = 0.05 \text{ s}^{-1}$  and  $0.1 \text{ s}^{-1}$  for the two pMHC and  $KT \gg 1$  for both, the initial activation rates per pMHC would be  $4.9 \times 10^{-5} \text{ s}^{-1}$  and  $1.7 \times 10^{-6} \text{ s}^{-1}$ , respectively. Even if there were a thousand peptides per APC, the agonist pMHC,  $k_{-1} = 0.05 \text{ s}^{-1}$ , would only activate on average one TCR every 20s. To get around this problem, McKeithan proposed (not shown in Fig. 6) that once the TCR had gone through  $N$  modifications and becomes activated, its half-life increases. This would allow the fully modified TCR to build up over time and achieve higher sensitivity. One problem with this proposal is that such a mechanism would inhibit serial engagement. In what follows we ignore the possibility of a change in the half-life of a pMHC-TCR complex when a TCR is fully modified since we know of no evidence that indicates this occurs.

By differentiating Eq. (4) with respect to  $k_{-1}$  and assuming that  $KT \gg 1$ , we find the value of  $k_{-1}$  where the rate of activation is maximal, is given approximately by  $k_{-1}^{\text{max}} = k_p/(N-1)$ . We expect  $k_{-1}^{\text{max}}$  to correspond to a dissociation rate for strong agonist peptides, about  $0.01 \text{ s}^{-1}$ . For the expression

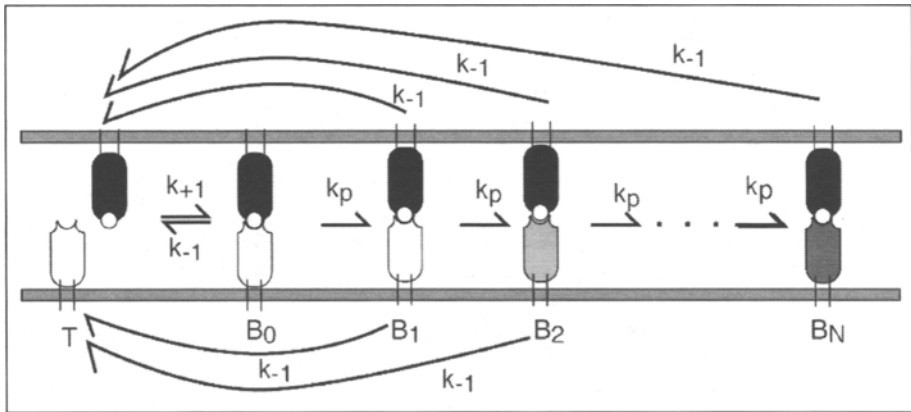


Figure 7. Kinetic proofreading model.  $T$  is the concentration of unbound TCR,  $B_0$  is the concentration of bound TCRs that have not been modified and  $B_i$  is the concentration of TCRs that have undergone  $i$  modifications. Each modification occurs with the same rate constant  $k_p$ . When a TCR has gone through  $N$  modifications, it is activated.

for  $k_{-1}^{\max}$  to be a reasonable approximation, we need  $KT > 1$ . For T-cells with 50,000 TCR per cell and a surface area of  $800 \mu\text{m}^2$  this requires that  $K > 1.6 \times 10^{-9} \text{cm}^2$ . For some but not all agonist peptide-MHC-TCR complexes, this inequality is satisfied.<sup>45</sup> From Eq. (2) we see that in this limit  $\text{hits/s} = k_{-1}$  and the rate limiting step in serial engagement is the breaking of the pMHC-TCR complex. Once a pMHC is free it rapidly finds a new TCR and binds to it.

To show that there is an optimal range of half-lives for cytotoxic T-lymphocyte (CTL) activation, Kalergis et al<sup>46</sup> used a series of  $\text{CD8}^+$  T-cell hybridomas expressing the wild type TCR and TCRs that had point mutations in their CDR3 $\beta$  domain and bound a VSV peptide-MHC with differing affinities. Using the same system, similar results were observed for the downregulation of TCR.<sup>44</sup> If these results arise from competition between kinetic proofreading and serial engagement, then the model predicts that going to high pMHC densities on the APC surface should remove the need for serial engagement in T-cell activation and an optimal range of half-lives for activation should no longer be observed. Consistent with this prediction, it was observed that when pMHC was present at high density, T-cell activation no longer went through a maximum as a function of the pMHC-TCR half-life but became a monotonic increasing function that reached a plateau for long half-lives.<sup>47</sup>

A problem with these studies is that the half-lives were not determined directly or at the same temperature that activation was measured. Rather the half-lives of pMHC-tetramers were measured at  $4^\circ\text{C}$  and it was assumed that the order of the half-lives was unchanged for the pMHC-monomers at  $25^\circ\text{C}$ . Whether the same ordering of half-lives occurs at  $25^\circ\text{C}$  is unknown. Holler and Kranz<sup>48</sup> used T-cells transfected with normal and engineered TCRs that had a wide range of pMHC-TCR half-lives and determined their half-lives and affinities at  $25^\circ\text{C}$ . They observed that T-cell activation was a monotonic increasing function of affinity that reached a plateau as a function of the pMHC-TCR half-life. They detected no optimal lifetime for the pMHC-TCR complex. Consistent with their results, Weber et al<sup>49</sup> engineered high affinity TCRs with slower off rates (also faster on rates) and found that the cognate peptide acted as a strong agonist for T-cells that had been transfected with these TCRs.

The evidence for pMHC serially engaging multiple TCRs at low peptide densities is compelling<sup>41,45,50</sup> as is the evidence for kinetic proofreading occurring in MIRR signaling.<sup>6</sup> As discussed, it has been proposed that at low pMHC densities TCR activation is a result of competition between these two effects and should result in TCR activation increasing to a maximum value and declining as a function of the pMHC-TCR complex lifetime. For interleukin 2 (IL-2) production, Kalergis

et al<sup>46</sup> observed an optimal range of half-lives for TCR activation while Holler and Kranz<sup>48</sup> did not. IL-2 production is a late response with many signal events occurring between pMHC-TCR binding and IL-2 production. To help resolve the question of whether competition occurs during signaling and leads to an optimal half-life for pMHC-TCR complex-triggered responses, early responses such as the activation of ZAP70 or the phosphorylation of LAT would make a much better target for study. As yet these studies have not been done.

## Concluding Remarks

Kinetic proofreading is an intrinsic property of the cell signaling process. It arises as a consequence of the multiple interactions that occur after a ligand triggers a receptor to initiate a signaling cascade and it ensures that false signals do not propagate to completion. An important consequence of kinetic proofreading is that it prevents signal propagation in the basal state due to fluctuations in the density of receptors (Faeder and Goldstein, unpublished results). In its basal state, a cell with receptors diffusing over its surface will always have some receptors close enough together that if one of the receptors is a PTK or associated with a PTK it can transphosphorylate its neighbor. Low levels of receptor phosphorylation occur in the absence of cognate ligands, but this phosphorylation does not generate a cellular response unless the receptors are overexpressed. Similarly, kinetic proofreading allows quality-controlled responses to the various ligands that a receptor can bind. Signals initiated by ligands with short binding half-lives are arrested at an early stage. This is particularly important for the MIRRs because either directly (the T-cell and B-cell receptors) or indirectly (the Fc receptors) they bind ligands with widely varying half-lives. It is therefore not surprising that kinetic proofreading was first introduced to cell-surface receptor signaling in this context and that the MIRRs have become the testing-ground for understanding the details of the manifestation of kinetic proofreading. There is considerable work still to be done.

## Acknowledgements

The work was supported by grants R37GM35556 and RR18754 from the National Institutes of Health and by the Department of Energy through contract DE-AC52-06NA25396.

## References

1. Reth M. Antigen receptor tail clue. *Nature* 1989; 338:383-384.
2. Cambier JC. Antigen and Fc receptor signaling: The awesome power of the immunoreceptor tyrosine-based activation motif (ITAM). *J Immunol* 1995; 155:3281-2185.
3. Hopfield JJ. Kinetic proofreading: A new mechanism for reducing errors in biosynthetic processes requiring high specificity. *Proc Natl Acad Sci USA* 1974; 71:4135-4139.
4. Hopfield JJ, Yamane T, Yue V et al. Direct experimental evidence for kinetic proofreading in amino acylation of tRNA<sup>Ala</sup>. *Proc Natl Acad Sci USA* 1976; 73:1164-1168.
5. McKeithan TW. Kinetic Proofreading in T-cell receptor signal-transduction. *Proc Natl Acad Sci USA* 1995; 92:5042-5046.
6. Torigoe C, Inman JK, Metzger H. An unusual mechanism for ligand antagonism. *Science* 1998; 281:568-572.
7. Faeder JR, Hlavacek WS, Reischl I et al. Investigation of early events in FcεRI-mediated signaling using a detailed mathematical model. *J Immunol* 2003; 170:3769-3781.
8. Wofsy C, Kent UM, Mao SY et al. Kinetics of tyrosine phosphorylation when IgE dimers bind to Fcε Receptors on rat basophilic leukemia-cells. *J Biol Chem* 1995; 270:20264-20272.
9. Wofsy C, Torigoe C, Kent UM et al. Exploiting the difference between intrinsic and extrinsic kinases: Implications for regulation of signaling by immunoreceptors. *J Immunol* 1997; 259:5984-5992.
10. Torigoe C, Goldstein B, Wofsy C et al. Shuttling of initiating kinase between discrete aggregates of the high affinity receptor for IgE regulates the cellular response. *Proc Natl Acad Sci USA* 1997; 94:1372-1377.
11. Yamashita T, Mao SY, Metzger H. Aggregation of the high-affinity IgE receptor and enhanced activity of P53/56(Lyn) protein-tyrosine kinase. *Proc Natl Acad Sci USA* 1994; 91:11251-11255.
12. Vonakis BM, Haleem-Smith H, Benjamin P et al. Interaction between the unphosphorylated receptor with high affinity for IgE and Lyn kinase. *J Biol Chem* 2001; 276:1041-1050.
13. Kihara H, Siraganian RP. Src homology 2 domains of Syk and Lyn bind to tyrosine-phosphorylated subunits of the high affinity IgE receptor. *J Biol Chem* 1994; 269:22427-22432.

14. Chen T, Repetto B, Chizzonite R et al. Interaction of phosphorylated FcεRIγ immunoglobulin receptor tyrosine activation motif-based peptides with dual and single SH2 domains of p72syk: Assessment of binding parameters and real time binding kinetics. *J Biol Chem* 1996; 271:25308-25315.
15. El-Hillal O, Kurosaki T, Yamamura H et al. Syk kinase activation by a src kinase-initiated activation loop phosphorylation chain reaction. *Proc Natl Acad Sci USA* 1997; 94:1919-1924.
16. Keshvara LM, Isaacson CC, Yankee TM et al. Syk- and Lyn-dependent phosphorylation of Syk on multiple tyrosines following B-cell activation includes a site that negatively regulates signaling. *J Immunol* 1998; 161:5276-5283.
17. Zhang J, Kimura T, Siraganian RP. Mutations in the activation loop tyrosines of protein tyrosine kinase Syk abrogate intracellular signaling but not kinase activity. *J Immunol* 1998; 161:4366-4374.
18. Siraganian RP, Zhang J, Suzuki K et al. Protein tyrosine kinase Syk in mast cell signaling. *Mol Immunol* 2002; 38:1229-1233.
19. Pribluda VS, Pribluda C, Metzger H. Transphosphorylation as the mechanism by which the high-affinity receptor for IgE is phosphorylated upon aggregation. *Proc Natl Acad Sci USA* 1994; 91:11246-11250.
20. Kent UM, Mao S-Y, Wofsy C et al. Dynamics of signal transduction after aggregation of cell-surface receptors: Studies on the type I receptor for IgE. *Proc Natl Acad Sci USA* 1994; 91:3087-3091.
21. Bunnell SC, Hong DI, Kardon JR et al. T-cell receptor ligation induces the formation of dynamically regulated signaling assemblies. *J Cell Biol* 2002; 158:1263-1275.
22. Mao SY, Metzger H. Characterization of protein-tyrosine phosphatases that dephosphorylate the high affinity IgE receptor. *J Biol Chem* 1997; 272:14067-14073.
23. Blinov ML, Faeder JR, Goldstein B et al. BioNetGen: Software for rule-based modeling of signaling transduction based on the interactions of molecular domains. *Bioinformatics* 2004; 20:289-291.
24. Faeder JR, Blinov ML, Goldstein B et al. Ruled-based modeling of biochemical networks. *Complexity* 2005; 10:22-41.
25. Faeder JR, Blinov ML, Goldstein B et al. Combinatorial complexity and dynamical restriction of network flows in signal transduction. *Syst Biol* 2005; 2:5-15.
26. Liu Z-J, Haleem-Smith H, Chen H et al. Unexpected signals in a system subject to kinetic proofreading. *Proc Natl Acad Sci USA* 2001; 98:7289-7294.
27. Saitoh S, Arudchandran R, Manetz TS et al. LAT is essential for FcεRI-mediated mast cell activation. *Immunity* 2000; 12:525-535.
28. Pierce M, Metzger H. Detergent-resistant microdomains offer no refuge for proteins phosphorylated by the IgE receptor. *J Biol Chem* 2000; 275:34976-34982.
29. Zhang W, Triple RP, Samelson LE. LAT palmitoylation: Its essential role in membrane microdomain targeting and tyrosine phosphorylation during T-cell activation. *Immunity* 1988; 9:239-246.
30. Field KA, Holowka D, Baird B. FcεRI-mediated recruitment of p53/56-lyn to detergent-resistant membrane domains accompanies cellular signaling. *Proc Natl Acad Sci USA* 1995; 92:9201-9205.
31. Field KA, Holowka D, Baird B. Compartmentalized activation of the high affinity immunoglobulin E receptor within membrane domains. *J Biol Chem* 1997; 272:4276-4280.
32. Rivera J, Cordero JR, Furumoto Y et al. Macromolecular protein signaling complexes and mast cell responses: A view of the organization of IgE-dependent mast cell signaling. *Mol Immunol* 2002; 38:1253-1258.
33. Wilson BS, Steinberg SL, Liederman K et al. Markers for detergent-resistant lipid rafts occupy distinct and dynamic domains in native membranes. *Mol Biol Cell* 2004; 15:2580-2592.
34. Rosette C, Werlen G, Daniels MA et al. The impact of duration versus extent of TCR occupancy on T-cell activation: A revision of the kinetic proofreading model. *Immunity* 2001; 15:59-70.
35. Eglite S, Morin JM, Metzger H. Synthesis and Secretion of monocyte chemoattractant protein-1 stimulated by high affinity receptor for IgE. *J Immunol*. 2003; 170:2680-2687.
36. Hlavacek WS, Redondo A, Metzger H et al. Kinetic proofreading models for cell signaling predict ways to escape kinetic proofreading. *Proc Natl Acad Sci USA* 2001; 98:7295-7200.
37. Hlavacek WS, Redondo A, Wofsy C et al. Kinetic proofreading in receptor-mediated transduction of cellular signals. *Bull Math Biol* 2002; 64:887-811.
38. Goldstein B, Faeder JR, Hlavacek WS. Mathematical models of immune receptor signaling. *Nat Rev Immunol* 2004; 4:445-456.
39. Coombs D, Goldstein B. T-cell activation: Kinetic proofreading, serial engagement and cell adhesion. *J of Computation and Appl Math* 2005; 184:121-139.
40. Krogsgaard M, Li Q-J, Sumen C et al. Agonist/endogenous peptide-MHC heterodimers drive T-cell activation and sensitivity. *Nature* 2005; 434:238-243.
41. Valitutti S, Muller S, Cella M et al. Serial triggering of many T-cell receptors by a few peptide-MHC complexes. *Nature* 1995; 375:148-151.

42. Lanzavecchia A, Lezzi G, Viola A. From TCR engagement to T-cell activation: A kinetic view of T-cell behavior. *Cell* 1999; 96:1-4.
43. van den Berg HA, Rand DA, Burroughs NJ. A reliable and safe T-cell repertoire based on low-affinity T-cell receptors. *J Theor Biol* 2001; 209:465-486.
44. Coombs D, Kalergis AM, Nathenson SG et al. Activated TCR remain marked for internalization after dissociation from peptide-MHC. *Nature Immunol* 2002; 3:926-931.
45. Wofsy C, Coombs D, Goldstein B. Calculations show substantial serial engagement of T-cell receptors. *Biophys J* 2001; 80:606-612.
46. Kalergis AM, Boucheron N, Doucey M-A et al. Efficient T-cell activation requires an optimal dwell-time of interaction between the TCR and the pMHC complex. *Nature Immunol* 2001; 2:229-234.
47. Gonzalez PA, Carreno LJ, Coombs D et al. Effects of pMHC and TCR dwell time on T-cell activation. *Proc Natl Acad Sci USA* 2005; 102:4824-4829.
48. Holler PD, Kranz DM. Quantitative analysis of the contribution of TCR/pepMHC affinity and CD8 to T-cell activation. *Immunity* 2003; 18:255-264.
49. Weber KS, Donermeyer DL, Allen PM et al. Class II-restricted T-cell receptor engineered in vitro for higher affinity retains peptide specificity and function. *Proc Natl Acad of Sci USA* 2005; 102:19033-19038.
50. Itoh Y, Hemmer B, Martin R et al. Serial TCR engagement and down-modulation by peptide: MHC molecule ligands: Relationship to the quality of individual TCR signaling events. *J Immunol* 1999; 162:2073-2080.
51. Torigoe C, Song JM, Barisas BG et al. The influence of actin microfilaments on signaling by the receptor with high-affinity for IgE. *Mol Immunol* 2004; 41:817-829.
52. Torigoe C, Faeder JR, Oliver JM et al. Kinetic proofreading of ligand-FcεRI interactions may persist beyond LAT phosphorylation. *J Immunol* 2007; 178:3530-3535.